Electronic Supplementary Material (ESI) for Dalton Transactions.
This journal is © The Royal Society of Chemistry 2021

Supporting Information

The tris-oxovanadium pyrogallate complex: synthesis, structure, magnetic and electronic properties

Hassan Mkhadder,[a] *Morgane Denis,*[a] *Mónica Giménez-Marqués,*[b] *Walter Cañón-Mancisidor,*[c] *Bernard Humbert,*[a] *Elise Deunf,*[a] *Philippe Poizot,*[a] *and Thomas Devic* *[a]

[a] Université de Nantes, CNRS, Institut des Matériaux Jean Rouxel, IMN, Nantes, France. Email : thomas.devic@cnrs-imn.fr.

[b] Instituto de Ciencia Molecular (ICMol), c/Catedrático José Beltrán, 2, 46980 Paterna, Spain.

[c] Facultad de Ingeniería, Ciencia y tecnología, Depto. Matemáticas y Ciencias de la Ingeniería, Universidad Bernardo O'Higgins, Chile.

[d] Centro de Nanociencia y Nanotecnología CEDENNA, Chile.

1. Synthesis

All reactants were obtained from commercial sources and used as received. As discussed in the manuscript, various experimental parameters we systematically screened with the final aim at producing samples suitable for single crystals XRD analysis. The optimized synthesis conditions are given below.

$K_3V_3O_3(pgal)_3 \bullet 2DMF$

100 mg (0.8 mmol, 1eq.) of H_3pgal, 210 mg (0.8 mmol; 1eq.) of VO(acac)$_2$, 0.158 mL (1.58 mmol, 2 eq.) of an aqueous 10 M KOH solution and 5 mL of N,N-dimethylformamide (DMF) were mixed in a 24 mL Teflon lined autoclave reactor. The reactor was sealed and heated at 120°C for 72 hours. After cooling down to room temperature, the dark solid was recovered by filtration, washed with DMF and dried in air.

$K_3V_3O_3(pgal)_3 \bullet 4H_2O$

100 mg (0.8 mmol, 1eq.) of H_3pgal, 210 mg (0.8 mmol; 1eq.) of VO(acac)$_2$, 0.317 mL (1.58 mmol, 2 eq.) of an aqueous 5 M KOH solution and 5 mL of methanol were mixed in a 12 mL glass vial. The reactor was sealed and heated at 60°C for 16 hours. After cooling down to room temperature, the dark solid was recovered by filtration, washed with methanol and dried in air.

2. X-ray diffraction (XRD) analysis

X-ray powder diffraction patterns were measured using a Bruker D8 Advance diffractometer with a Bragg-Brentano geometry producing Cu Kα radiation and equipped with a LynxEye detector, or an INEL XRG3500 diffractometer with a Debye-Scherrer geometry producing Cu K radiation. Extractions from the peak positions, pattern indexing and whole powder pattern indexing without crystal structural model were carried out with the Fullprof suite.[1] The final plots are shown Figure 2a, and the deduced cell parameters given Table S1.

Table S1. Comparison of the unit-cell parameters refined form the powder (P) and single crystal (SC) X-ray diffraction experiments (PXRD and SCXRD respectively).

Compound		**a (Å)**	**b (Å)**	**c (Å)**	**β (°)**	**V (Å^3)**
$K_3V_3O_3(pgal)_3$•$4H_2O$ monoclinic, *P*2_1/*c*	SC	13.734(3)	14.379(3)	15.837(3)	114.68(3)	2842(1)
	P	13.692(4)	14.302(4)	15.854(3)	114.83(2)	2818(1)
$K_3V_3O_3(pgal)_3$•2DMF monoclinic, *P*2_1/*n*	SC	8.1630(3)	26.1908(8)	15.0823(4)	104.210(3)	3125.9(2)
	P	8.207(2)	26.053(7)	15.163(4)	104.40(1)	3140(1)

Crystal data of $K_3V_3O_3(pgal)_3$•$4H_2O$ was analyzed at room temperature using a Bruker-Nonius Kappa CCD diffractometer working at the Mo Kα radiation. The Bruker AXS "Collect" suite was used to integrate and scale intensities and a semi-empirical absorption correction (SADABS) were applied on the basis of multiple scans of equivalent reflections. For the DMF solvate $K_3V_3O_3(pgal)_3$•2DMF, only microcrystals could be obtained. Data were thus collected on the Cristal beamline at Synchroton Soleil, using a set up adapted for small crystals at 100(2) K on an Xcalibur, Atlas four-circle diffractometer and equipped with a CCD plate detector. Data reduction was performed using CrysAlis. An empirical absorption correction was applied using spherical harmonics on the basis of multiple scans of equivalent reflections, implemented in SCALE3 ABSPACK scaling algorithm. Both structures were solved by direct methods using SHELXS and refined with the full matrix least squares routine SHELXL.[2] Non H-atoms were refined anisotropically, except two water molecules (OW3 and OW4) in the hydrated solid. These molecules were found to be disordered over two positions (A and B), whose occupancies were refined to 58 and 42 % respectively. H atoms were added as rigid bodies except one the water molecules for $K_3V_3O_3(pgal)_3•4H_2O$. The content of the unit-cells is shown Figure S1. Note that both solids are prone to slow (~days) desolvatation.

CCDC 2087736 ($K_3V_3O_3(pgal)_3•4H_2O$) and 2087735 ($K_3V_3O_3(pgal)_3•2DMF$) contain the supplementary crystallographic data for this paper. These data can be obtained free of charge from the Cambridge Crystallographic Data Centre via http://www.ccdc.cam.ac.uk/Community/Requestastructure. Crystallographic and refinements parameters are summarized in Table S1.

Table S1. Crystallographic data and refinement parameters for $K_3V_3O_3(pgal)_3•2DMF$ and $K_3V_3O_3(pgal)_3•4H_2O$.

Compound	**$K_3V_3O_3(pgal)_3•2DMF$**	**$K_3V_3O_3(pgal)_3•4H_2O$**
Empirical formula	$C_6H_6N_4O_6$	$C_{12}H_{18}ClLaN_6O_8$
Formula weight (g·mol^{-1})	833.57	759.43
Temperature (K)	100(2)	293(2)
Wavelength (Å)	0.67173	0.71073
Crystal system	monoclinic	monoclinic
Space group	$P2_1/n$	$P2_1/c$
Unit cell dimensions (Å)	a = 8.1630(3) b = 26.1908(8) c = 15.0823(4) β = 104.210(3)°	a = 13.734(3) b = 14.379(3) c = 15.837(3) β = 114.68(3)°
Volume (Å^3)	3125.9(2)	2842(1)
Z, calculated density (g·cm^3)	4, 1.771	4, 1.775
Adsorption coefficient (mm^{-1})	1.142	1.476
F(000)	1676	1516
Crystal size (mm^3)	0.04 x 0.03 x 0.02	0.30 x 0.25 x 0.08
Theta range for data collection	2.568° - 26.604°	2.611° - 27.103°
Limiting indices	$-9 \leq h \leq 9$ $-34 \leq k \leq 34$ $-20 \leq l \leq 20$	$-16 \leq h \leq 17$ $-18 \leq k \leq 18$ $-20 \leq l \leq 20$

Reflections collected / unique	34565/7285 [R(int) = 0.0599]	74041/6277 [R(int) = 0.0553]
Refinement method	full-matrix least squares	
Data / Restraints / Parameters	7285/0/419	6277/0/360
Goodness of fit on F^2	1.034	1.075
Final R indices [I > 2σ(I)]	R1 = 0.0426 wR2 = 0.919	R1 = 0.0659 wR2 = 0.1606
R indices (all data)	R1 = 0.0707 wR2 = 0.1035	R1 = 0.1137 wR2 = 0.877
Largest diff peak and hole (e·Å^{-3})	0.501 and -0.518	1.001 and -0.456

Table S2. V-O bond distances and the corresponding valences deduced from [3]; calculations were carried using the bond valence parameters of V(III), V(IV) and V(V), and confirm a +IV oxidation state for all vanadium cations in both structures.

V-O distance (Å)			Valence		
			hyp. V(III)	*hyp. V(IV)*	*hyp. V(V)*
$K_3V_3O_3(pgal)_3\cdot 2DMF$					
V3	O24	1.618(2)	1.40	1.57	1.65
	O3	1.955(2)	0.56	0.63	0.66
	O21	1.958(2)	0.56	0.63	0.66
	O2	2.019(2)	0.47	0.53	0.56
	O22	2.030(2)	0.46	0.51	0.54
		sum	**3.46**	**3.87**	**4.07**
V1	O4	1.617(2)	1.41	1.57	1.65
	O13	1.947(2)	0.55	0.61	0.65
	O1	1.970(2)	0.55	0.62	0.64
	O2	2.013(2)	0.48	0.54	0.57
	O12	2.046(2)	0.44	0.49	0.52
		sum	**3.42**	**3.83**	**4.03**
V2	O14	1.612(2)	1.43	1.59	1.68
	O23	1.954(2)	0.57	0.63	0.66
	O11	1.975(2)	0.53	0.60	0.63
	O12	2.024(2)	0.47	0.52	0.55
	O22	2.037(2)	0.45	0.50	0.53
		sum	**3.44**	**3.85**	**4.05**
$K_3V_3O_3(pgal)_3\cdot 4H_2O$					
V1	O4	1.600(4)	1.47	1.65	1.73
	O1	1.953(4)	0.57	0.63	0.67
	O11	1.962(4)	0.55	0.62	0.65
	O12	2.001(4)	0.50	0.56	0.59

	O2	2.002(4)	0.50	0.55	0.58
		sum	**3.59**	**4.00**	**4.22**
V2	O14	1.608(4)	1.44	1.61	1.69
	O21	1.940(4)	0.59	0.66	0.69
	O13	1.948(4)	0.57	0.64	0.68
	O12	2.001(4)	0.50	0.56	0.59
	O22	2.008(4)	0.49	0.55	0.57
		sum	**3.59**	**4.01**	**4.22**
V3	O24	1.598(5)	1.48	1.65	1.74
	O3	1.926(4)	0.61	0.68	0.71
	O23	1.950(4)	0.57	0.64	0.67
	O22	1.999(4)	0.50	0.56	0.59
	O2	2.001(4)	0.50	0.56	0.59
		sum	**3.66**	**4.08**	**4.30**

Table S3. Short (≤ 3.30 Å) K-O distances (Å).

	$K_3V_3O_3(pgal)_3\cdot 2DMF$	
K1	O41	2.681(3)
	O23	2.705(2)
	O11	2.708(2)
	O11	2.860(2)
	O14	3.000(2)
K2	O13	2.674(2)
	O3	2.765(2)
	O24	2.848(2)
	O1	2.880(2)
	O21	2.993(2)
	O31	3.106(3)
	O14	3.227(2)
	O4	3.335(2)
K3	O24	2.725(2)
	O13	2.732(2)
	O31	2.751(3)
	O21	2.865(2)
	O4	2.869(2)
	$K_3V_3O_3(pgal)_3\cdot 4H_2O$	
K1	OW2	2.668(5)
	O4	2.713(4)
	OW1	2.840(5)
	OW2	2.920(6)
	OW3B	2.97(2)

	O21	2.976(5)
	O14	2.988(5)
	OW4B	3.11(3)
	OW3A	3.18(3)
K3	O21	2.684(4)
	O11	2.801(4)
	O1	2.839(4)
	O13	2.904(5)
	O24	2.932(5)
	O4	3.055(4)
	O14	3.195(5)
	OW3A	3.30(4)
K2	O3	2.624(5)
	O23	2.746(5)
	O23	2.815(5)
	OW1	2.831(6)
	OW3B	2.89(2)
	O24	3.228(5)

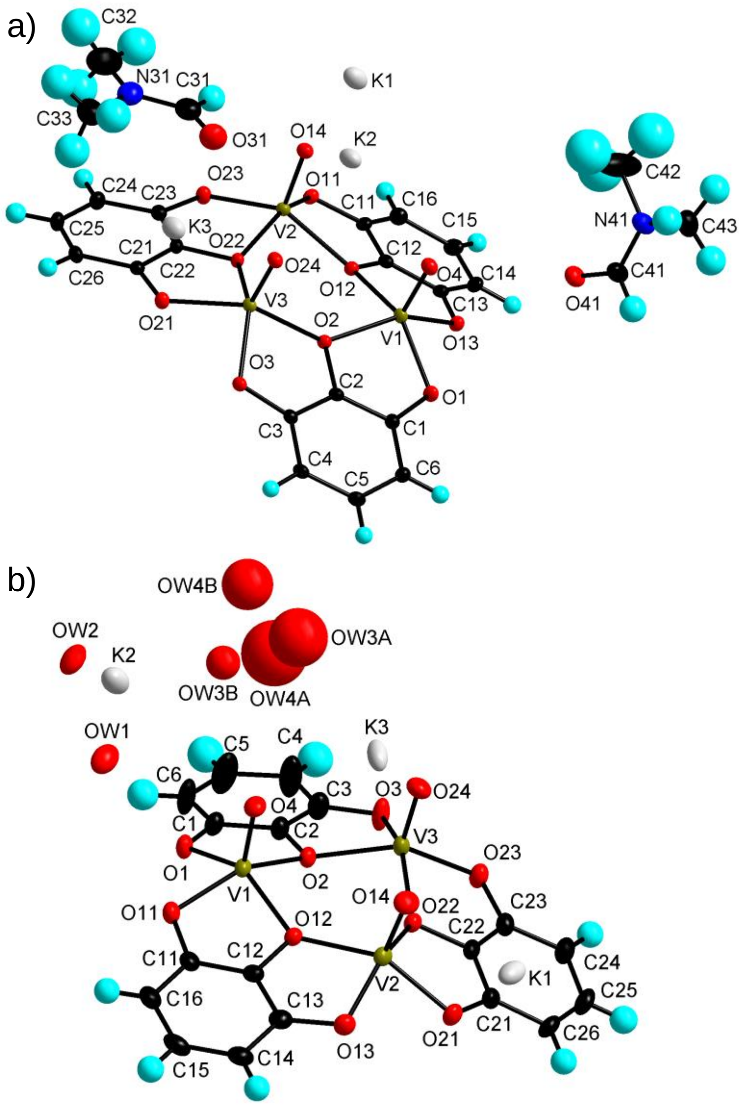

Figure S1. Content of the asymmetric unit of a) $K_3V_3O_3(pgal)_3 \cdot 2DMF$ and b) $K_3V_3O_3(pgal)_3 \cdot 4H_2O$. ADPs are shown at the 30% probability level.

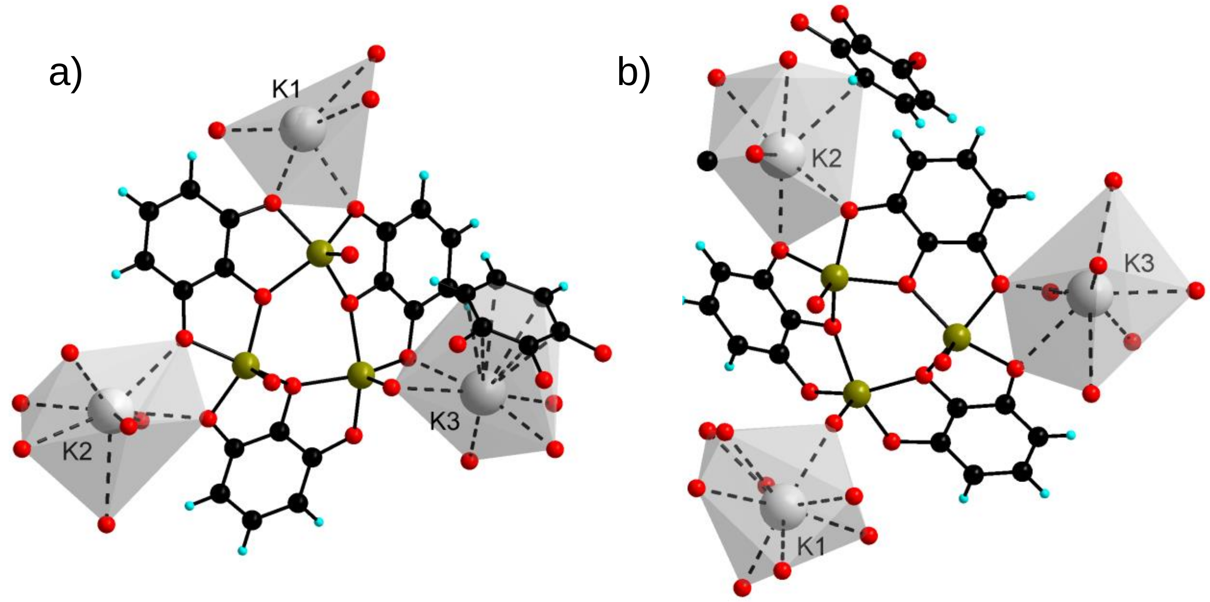

Figure S2. Environment of the potassium ions in a) $K_3V_3O_3(pgal)_3\cdot 2DMF$ and b) $K_3V_3O_3(pgal)_3\cdot 4H_2O$.

Table S4. Short (≤ 3.35 Å) K-C distances (Å). *Bound to an oxygen interacting with K^+.

	$K_3V_3O_3(pgal)_3\cdot 2DMF$	
K3	C1	3.155(3)
	C2	3.174(3)
	C3	3.317(3)
	C4	3.349(3)
	C5	3.293(3)
	C6	3.217(3)
K1	C11*	3.334(3)
	$K_3V_3O_3(pgal)_3\cdot 4H_2O$	
K2	C6	3.173(9)
	C23*	3.170(6)

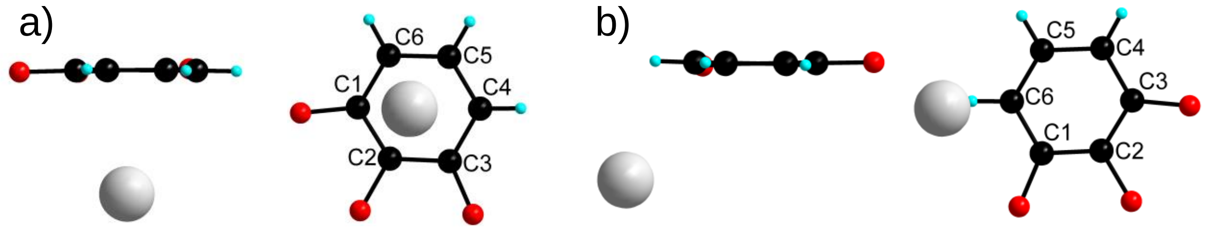

Figure S3. Short contacts between K^+ and pyrogallate rings, suggesting the occurrence of K^+-π interactions. a) K3 in $K_3V_3O_3(pgal)_3{\cdot}2DMF$ and b) K2 in $K_3V_3O_3(pgal)_3{\cdot}4H_2O$.

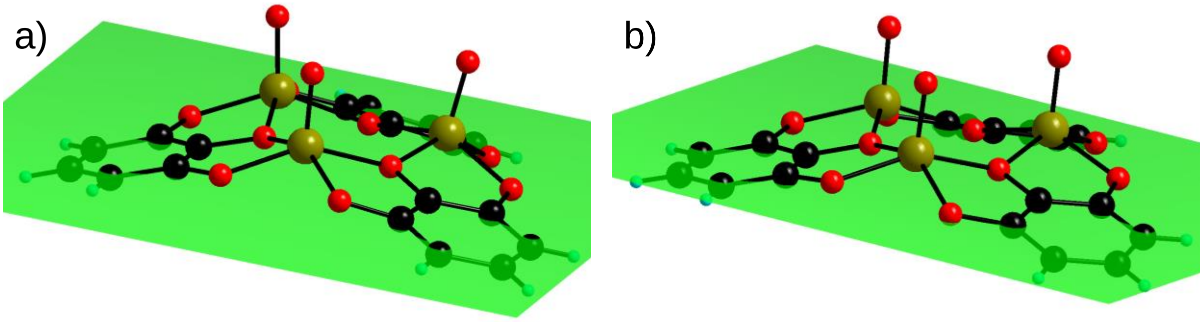

Figure S4. View of the trimetallic complexes in a) $K_3V_3O_3(pgal)_3{\cdot}2DMF$ and b) $K_3V_3O_3(pgal)_3{\cdot}4H_2O$. All vanadium ions lie 0.9 to 1.1 Å out of the mean planes defined by the three phenyls rings (shown in light green).

3. Vibrational spectroscopies

Infrared (IR) spectra were collected at room temperature on a Bruker Alpha spectrometer in the attenuated total reflectance (ATR) mode between 400 and 4000 cm^{-1}. Data are shown Figures 3a and S5.

Raman spectra were collected at room temperature on a Renishaw InVia upon excitation at 785 nm, both in the range 1720-620 and 620-60 cm^{-1}. Data are shown Figures 3b and S6.

Reflectance UV/Vis spectra were collected on a Perkin Elmer Lambda 1050 spectrophotometer, with the solid diluted in KBr. Data (see Figure 3c) were plotted in the form of normalized Kubelka-Munk functions using the equation: K-M = $(1-R)^2/2R$ with R = Reflectance.

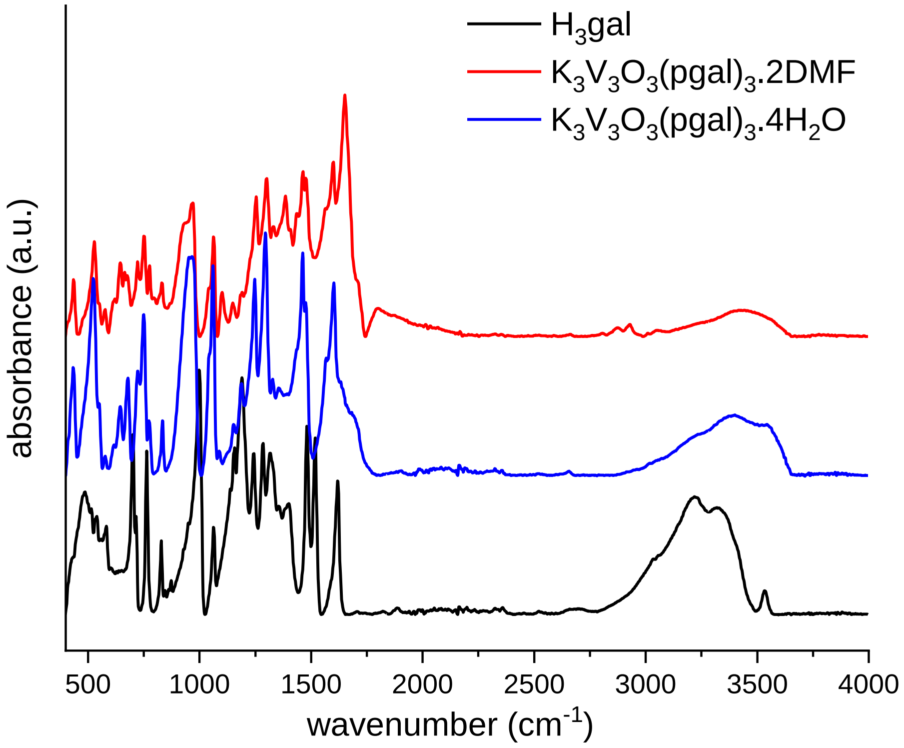

Figure S5. Infrared spectra of H_3pgal (black), $K_3V_3O_3(pgal)_3\cdot2(DMF)$ (red) and $K_3V_3O_3(pgal)_3\cdot4(H_2O)$ (blue).

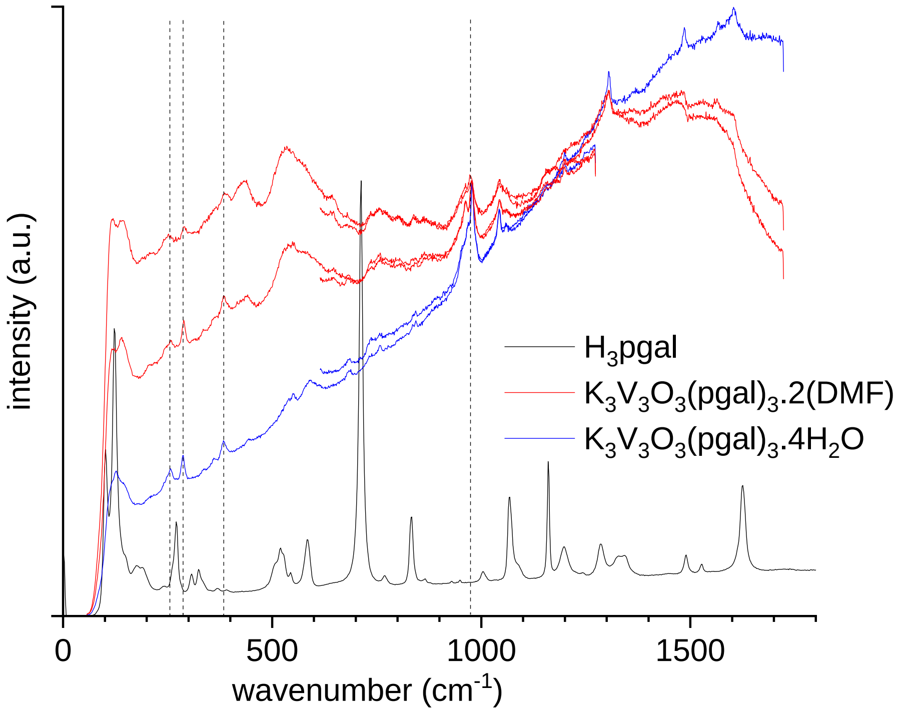

Figure S6. Raman spectra of H_3pgal, $K_3V_3O_3(pgal)_3\cdot2(DMF)$ and $K_3V_3O_3(pgal)_3\cdot4(H_2O)$.

4. Thermogravimetric analysis (TGA)

Thermogravimetric analyses (TGA) were performed on Mettler Toledo apparatus under O_2 atmosphere, at a heating rate of 5 K min^{-1} up to 700°C. TG curves are shown Figure 2b, and quantitative analysis of the data summarized Table S5. Calculation were carried out considering various amount of water molecules in the hydrate; n = 6 lead to the best agreement.

Table S5. Quantitative analysis of the TG results.

Compound	**$K_3V_3O_3(pgal)_3\cdot n(H_2O)$**		**$K_3V_3O_3(pgal)_3\cdot2(DMF)$**	
	weight (%)		*weight (%)*	
	exp.	*calc.*	*exp.*	*calc.*
solvated (room T).	100	100	100	100
desolvated (first plateau) $K_3V_3O_3(pgal)_3$	87	90 (n = 4) 86 (n = 6)	83	82

~$K^{I}V^{V}O_3$ (second plateau)	50	55 (n = 4) 52 (n = 6)	47	50

5. SEM-EDX

Energy-dispersive X-ray spectroscopy (EDXS) analysis was carried out on a JEOL JSM 5800LV microscope equipped with an energy dispersive SDD SAMx spectrometer working at 15 kV. Samples were pasted on carbon tape and further coated with carbon to improve the electronic conductivity. Data are shown Figure S7.

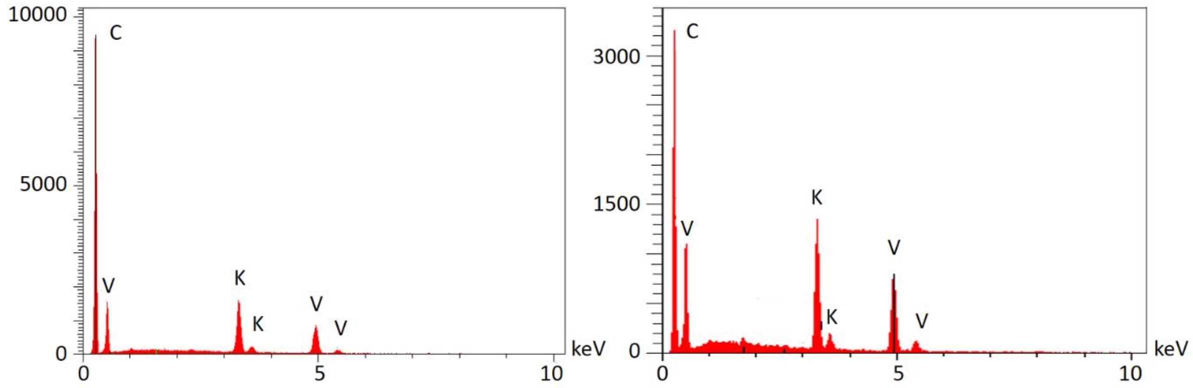

Figure S7. Energy-dispersive X-ray spectra of $K_3V_3O_3(pgal)_3{\cdot}4H_2O$ (left) and $K_3V_3O_3(pgal)_3{\cdot}2DMF$ (right). Derived K:V atomic ratio are 46:54 and 48:52 respectively.

6. Electrochemical assessments

Solid state electrochemical experiments were carried out by using a two-electrode Swagelok®-type cell using a Li metal disc as the negative electrode and a glassfiber separator soaked with 1 M $LiPF_6$ in a 1:1 mixture of ethylene carbonate (EC) and dimethylcarbonate (DMC) as the electrolyte. The composite positive electrode was prepared without a binder in an argon filled glovebox by grinding the powder of anhydrous $K_3V_3O_3(pgal)_3$ material (dried at 120°C under vacuum) and carbon additive (to insure proper electronic conduction (complex:carbon ratio =

75:25 wt%, ca. 3 mg of active material per electrode). Carbon black Ketjenblack® EC-600JD (Akzo Nobel) denoted KB600 was used for the anodic investigations whereas carbon black C-NERGY® Super C65 was preferred for the cathodic measurements. The electrochemical cells were then cycled in galvanostatic mode at a rate of C/10 (one electron exchanged per 1/3($K_3V_3O_3(pgal)_3$) in 10 hours) in the potential range 2.5-4.0 V or 2.8-3.7 V (starting in oxidation) and 1.0-3.0 V vs. Li^+/Li (starting in reduction) by using a MPG-2 multi-channel system (Bio-Logic SAS, Seyssinet-Pariset, France). The corresponding recorded data are shown Figures 4a and S8.

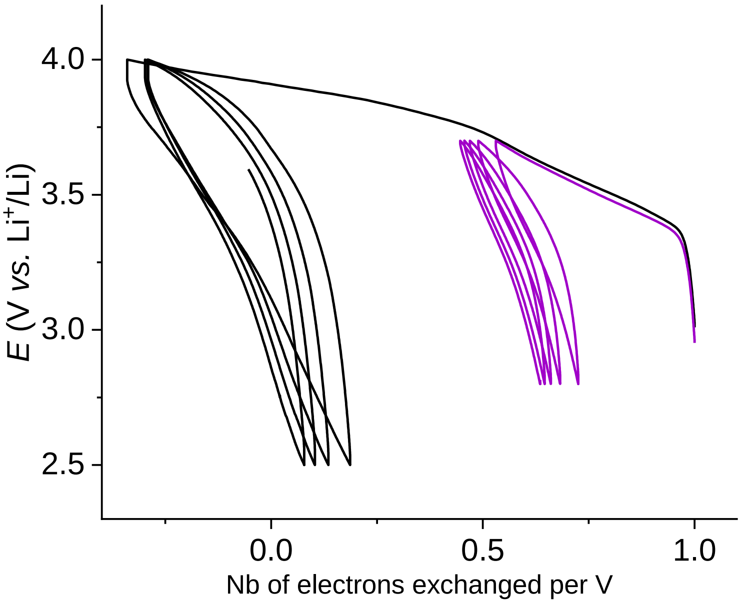

Figure S8. Electrochemical behavior of the $K_3VO_3(pgal)_3$ complex measured in the solid state (anhydrous phase) *vs.* Li by using a galvanostatic cycling method starting in oxidation for the potential windows 2.5-4.0 (black) and 2.8-3.7 V vs. Li^+/Li (purple), respectively. Electrolyte: 1 M $LiPF_6$ in EC/PC; cycling rate: C/10).

Cyclic voltammetry experiments performed in aqueous solution by using a standard 3-electrode glass cell. The working electrode was constituted of a commercial platinum disk microelectrode with a diameter of 1.6 mm (ALS Japan). Facing the working electrode, a large platinum wire (coil) was used as the counter electrode. An AgCl/Ag/KCl 3.5 M reference electrode was used.

Electrochemical measurements were performed by using a SP-300 potentiostat/galvanostat from Bio-logic SAS at a scan rate of 200 mV s^{-1}. A 1 M $MClO_4$ (M = Li, Na) aqueous solution was used as supporting electrolyte, and the concentration of complex was *ca.* 10^{-3} M. The corresponding recorded data are shown Figures 4b and S9-S10.

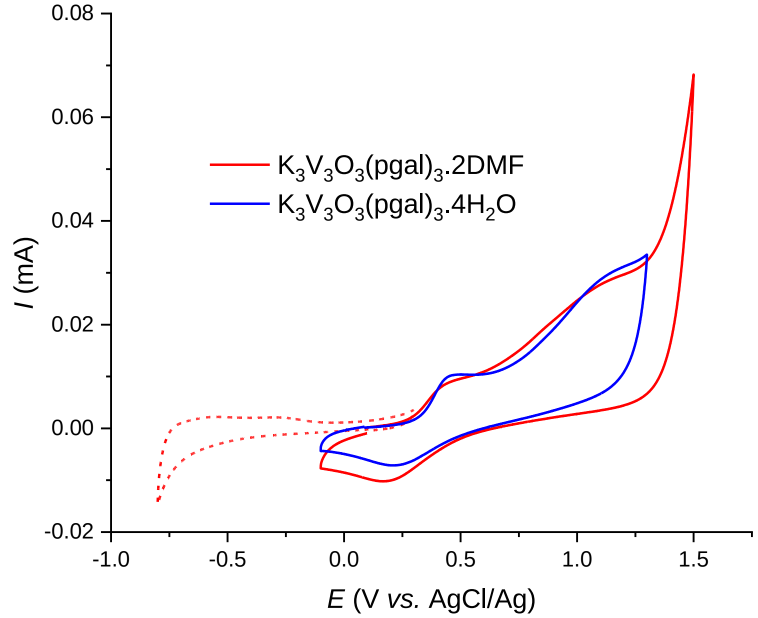

Figure S9. a) Comparison of the CV traces of $K_3V_3O_3(pgal)_3{\cdot}4H_2O$ and $K_3V_3O_3(pgal)_3{\cdot}2DMF$ dissolved in 1 M $LiClO_4$ aqueous electrolyte. The electrochemical activity of $K_3V_3O_3(pgal)_3{\cdot}2DMF$ in reduction is reported in dashed line.

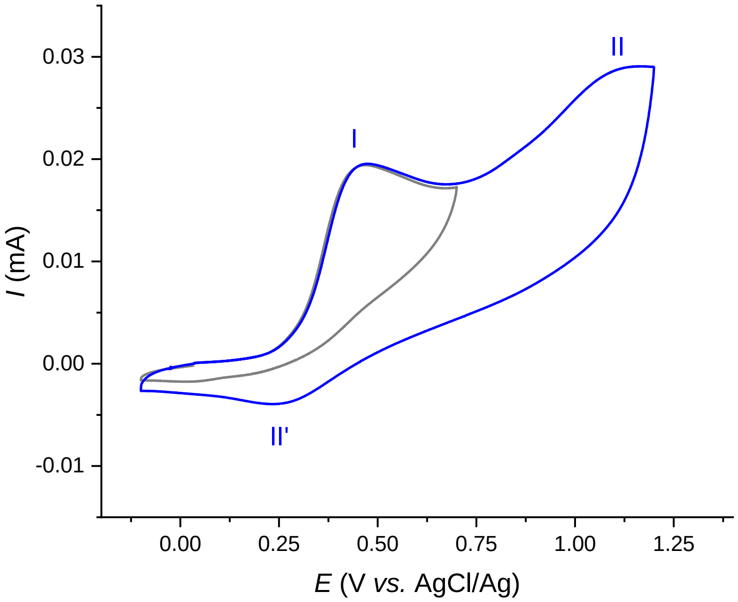

Figure S10. CV traces of $K_3V_3O_3(pgal)_3\cdot4H_2O$ dissolved in 1 M $NaClO_4$ in aqueous electrolyte within the potential range -0.2-0.7 V (grey) and -0.2-1.2 V vs. AgCl/Ag (blue), respectively. This experiment unambiguously indicates that the reduction peak at 0.25 V vs. AgCl/Ag is related to oxidation II and not I.

7. Magnetic properties

Magnetic measurements were performed on ground crystals of $K_3V_3O_3(pgal)_3\cdot4H_2O$ in a Quantum Design Physical Property Measurement System (PPMS). Variable temperature (2 - 300 K) direct current (*dc*) magnetic susceptibility measurements were carried out under an applied field of 1 kG, and variable field magnetization measurements up to 5 T were performed at 2.0 K for compound $K_3V_3O_3(pgal)_3\cdot4H_2O$. The susceptibility data were corrected for the diamagnetic contributions of the sample, using Pascal´s constants.[4]

Dynamic magnetic measurements (ac) upon the application of different dc fields (500-6000 G) show frequency-dependent signals in the out-of-phase (Figure S11), revealing that high dc fields are necessary to properly study the relaxation dynamics. Figure S11 depicts the appearance of frequency dependent signals in the out-phase susceptibility measuring at 5000 G and 6000 G dc fields.

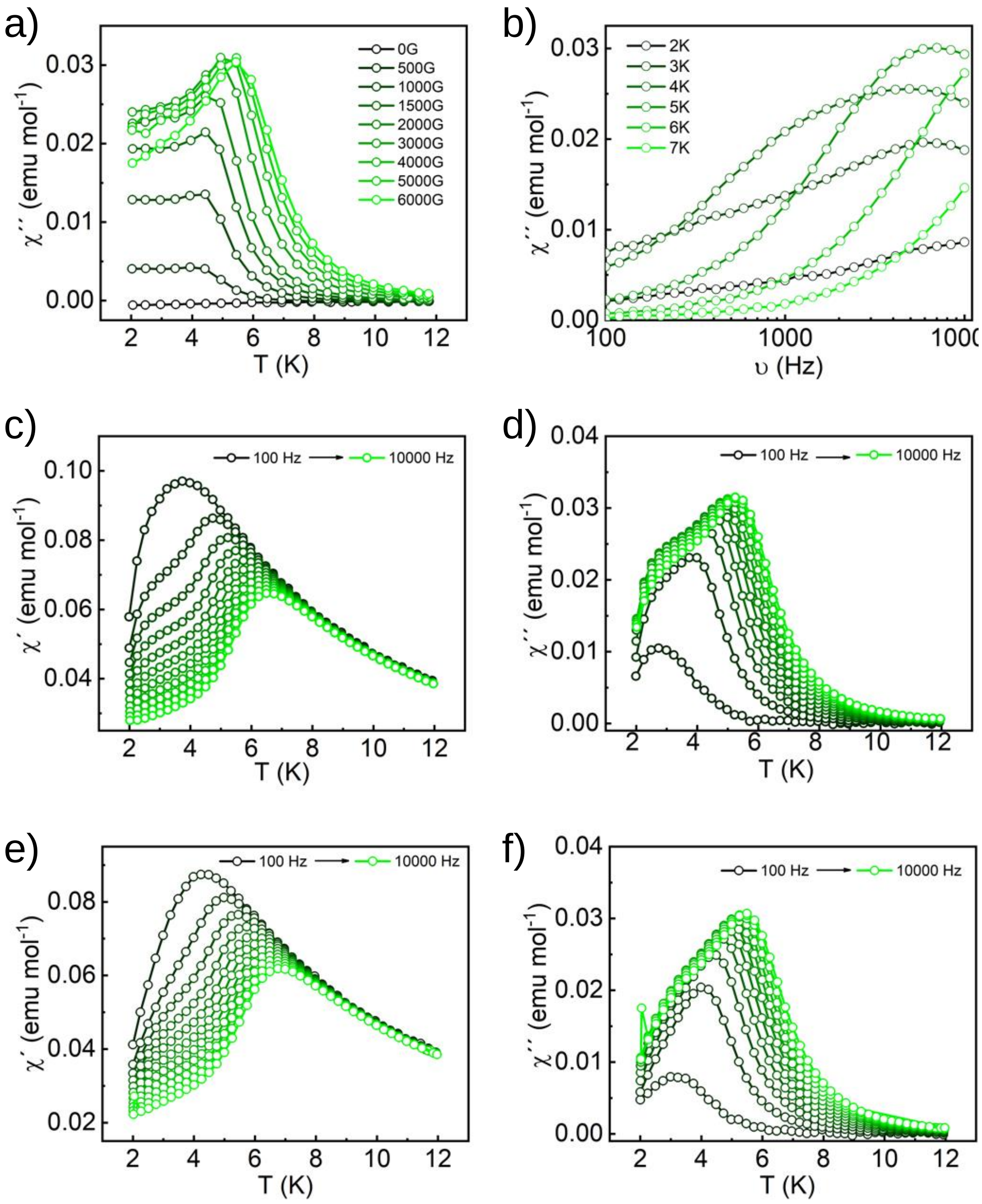

Figure S11. (a) ac susceptibility χ ´´(T) measurement at υ = 10000 Hz for $K_3V_3O_3(pgal)_3{\cdot}4H_2O$ and at different dc fields performed to obtain the optimal field to study the relaxation dynamics. (b) out-of-phase susceptibility measurements (χ ´´(υ)) at different temperatures under a dc magnetic field of 6000 G. (c-f) ac susceptibility (χ ´(T) and χ ´´(T)) measurements at different frequencies under an applied dc magnetic field of 5000 G (c, d) and 6000 G (e, f).

The relaxation dynamics were analyzed considering the Orbach process and separately, the Raman + direct relaxation mechanism.[5] The best fit parameters considering these mechanisms are shown Table S6.

Table S6. Best fit parameters of temperature dependence of the relaxation time of the ac magnetic susceptibility data measured at the two fields (5000 G and 6000 G).

	Orbach ($\tau = \tau_0 \cdot e^{U_{eff}/k_B T}$)		Raman + Direct ($\tau = A \cdot T + B \cdot T^n$)		
H_{dc}	U_{eff} (cm^{-1})	t_0 (s)	A (s^{-1} K^{-1})	B (s^{-1} K^{-n})	n
5000 G	15.23 (55)	2.21 (31) x 10^{-7}	0.45 (11)	0.13 (05)	6.7 (2)
6000 G	16.64 (34)	1.29(25) x 10^{-7}	0.37 (08)	0.046 (13)	7.2 (2)

References

---

[1] J. Rodriguez-Carjaval, *Physica B* **1993**, *192*, 55.

[2] G. Sheldrick, *Acta Crystallographica Section C* **2015**, *71*, 3-8.

[3] E. Brese, M. O’Keeffe, *Acta Cryst.* **1991**, *B47*, 192-197.

[4] G. A. Bain, J. F. Berry, *J. Chem. Educ.* **2008**, *85*, 532–536.

[5] L. Tesi, E. Lucaccini, I. Cimatti, M. Perfetti, M. Mannini, M. Atzori, E. Morra, M. Chiesa, A. Caneschi, L. Sorace, R. Sessoli, *Chem. Sci.* **2016**, *7*, 2074; M. Atzori, E. Morra, L. Tesi, A. Albino, M. Chiesa, L. Sorace, R. Sessoli, *J. Am. Chem. Soc.* **2016**, *138*, 11234.